TECHNICAL MEMORANDUMS

NATIONAL ADVISORY COMMITTEE FOR AERONAUTICS

No. 990

CONTRIBUTION TO THE AERODYNAMICS OF

ROTATING-WING AIRCRAFT

PART II

By G. Sissingh

Washington
October 1941

NATIONAL ADVISORY COMMITTEE FOR AERONAUTICS

TECHNICAL MEMORANDUM NO. 990

CONTRIBUTION TO THE AERODYNAMICS OF

ROTATING-WING AIRCRAFT*

PART II

By G. Sissingh

The interrelations established in an earlier report on this subject (NACA T.M. No. 921) are used to study the best assumptions for hovering and horizontal flight. The effect of the twisted and tapered blade on the rotor efficiency is analyzed and the gliding coefficient at different stages (from autogiro to helicopter) of horizontal flight compared. To the extent that model or full-scale test data are available, they are included in the comparison.

NOTATION

In addition to the notation employed in the earlier report (T.M. No. 921), the following symbols are used:

G (kg) tare weight of aircraft

N (hp) rotor input power

N_z (hp) input power of regular propeller on autogiro or helicogyro

v factor identifying the flight stage

$$v = \frac{N}{N + N_z}$$

$v = 0$ autogiro

$v = 1$ helicopter

$1 > v > 0$ helicogyro

η static-thrust efficiency: $\eta = \dfrac{k_{sa}^{3/2}}{2k_d} = M = .707 \dfrac{C_T^{3/2}}{C_Q}$

ϵ gliding coefficient of rotating-wing aircraft, rotor-gear efficiency, and efficiency of normal propeller equated to 1:

$$\epsilon = \frac{k_{sh} + f \lambda^2}{k_{sv}} + \frac{k_d}{\lambda \, k_{sv}}$$

with $\lambda = V/U \cong \mu$

f ratio of parasite area of all nonlifting parts of the aircraft to swept rotor-disk area F

$\sigma_{0.7}$ reduced solidity of a tapered blade; σ referred to blade chord at 0.7R

$$\sigma_{0.7} = \frac{z \, t_0 \, (1 + 0.7 \, p)}{\pi \, R}$$

GENERALITIES

Depending upon the purpose of use of the rotating-wing aircraft as load carrier, where the speed is secondary, or as air liner with high cruising speed – the principal value is placed on a high rotor lifting power or a good lift/drag ratio of the aircraft. However, since one requirement of a rotating-wing aircraft is its ability to take off and land vertically, the tare weight and the rotor power available decide the minimum diameter of the rotor disk. Decisive, finally, is the thrust per unit power, which follows at

$$G/N = 75 \, \eta \, \sqrt{\frac{2\rho}{G/F}} \quad \text{kg/hp} \tag{78}$$

As regards the static-thrust efficiency, η, it suffices to state that, for the present, it ranges from 60 to 75 percent and depends upon the aerodynamic design of the rotor.

According to equation (78) and figure 8, the lift capacity of a rotor increases with decreasing blade loading which, for modern airplanes of from about 800 to

1000 kilograms total weight, ranges from 6 to 10 kg/m², and more for larger and faster types.

Figure 9 illustrates the relation between diameter, total weight, and power according to equation (78), at $\eta = 0.7$ static-thrust efficiency. The diameter resulting from figure 9 would just suffice to keep the aircraft hovering without ground effect.* Obviously, a certain excess lift is necessary for climbing, etc., which requires a correspondingly greater diameter. Solving equation (78) with respect to D, affords

$$D = 0.01065 \; \frac{G^{3/2}}{\eta \, N \sqrt{\rho}} \tag{78a}$$

In other words, a desired percent of change of lift requires approximately 1.5 times the rotor diameter. At constant η, for instance, a 15-percent increase in diameter raises the lifting power 10 percent. But with consideration for the weight of the blades and the sag at static thrust**, this rotor enlargement cannot be continued arbitrarily.

Of further general importance is the circumferential speed at the tip circle, which on modern aircraft of the type Ar C 30 ranges from 100 to 150 meters per second and which - as shown later on - cannot be substantially changed for various reasons.

For estimated prediction of the best value, we quote the result of a subsequent calculation, which states that the best static thrust coefficient is secured by a blade loading of $k_{sa}/\sigma \cong 0.2$. With this value and D, according to equation (78a), the equation for the axial thrust $(G = k_{sa} \, F \, U^2 \, \frac{\rho}{2})$ gives as best tip speed in the hovering stage:

---

*In direct proximity of the ground, the thrust for equal power input is greater. This increase in lift is effective at a distance of 0.6 to 0.8 D between rotor disk and ground and can, for modern airplane types, amount to as much as 30 percent.

**To keep the blade stresses in flight to a minimum, they should be flexible in bending at right angles to the plane of rotation. In this manner, unloading from the centrifugal force makes it possible to lower the bending stress to about 20 percent of the inelastic blade.

$$U = \frac{335 \ \eta \ N}{G \ \sqrt{\sigma}} \ m/s \qquad (79)$$

Figure 10 gives the tip speed plotted against the power loading conformable to equation (79) for the practical solidity ratios $\sigma = 0.04$ to 0.10. It is pointed out on this occasion that, while high σ favors the static-thrust coefficient, the lower σ is more propitious for horizontal flight. Figure 10 shows the power loading referred to the total weight. To enable the rotor to carry n times this total weight, the tip speed must further be reduced in the ratio 1:n. The thus-secured U value considers only the hovering stage or the climb. If, in addition, the airplane is to have high speed in level flight, other viewpoints are involved which restrict the range considerably.

Since the drag coefficient for normal profiles increases materially when operating in proximity of sonic velocity, high Mach numbers must be avoided as much as possible (reference 1). The highest relative speed on the rotating-wing aircraft is at the tip of the advancing blade ($\psi = 90^\circ$), where flight and circumferential speed become additive. If it is assumed that the sum of these two speeds is not permitted to exceed a specified value, the flying speed will be maximum for each circumferential speed.

Figure 11 illustrates this connection for different coefficients of advance λ (ratio of flight to circumferential speed). The limit following the requirement of a maximum permissible Mach number is included on the basis that the highest relative speed at the blade tip is not to exceed 90 percent of the velocity of sound. Since this high speed is confined to a small part of the rotor disk, the permissible Mach number might perhaps be raised a little without appreciable detriment to the gliding coefficient of the rotor. Theoretically, this produces no change in the speed limitation of rotating-wing aircraft.

Since the efficiency decisive for horizontal forward flight, the gliding coefficient (of the rotating-wing aircraft), reaches its best value by a coefficient of advance $\mu = 0.35$ to 0.40, the speed limit of the best horizontal flight is, according to figure 11, about 300 kilometers per hour. Of course, by foregoing the minimum gliding coefficient, it is quite possible to design rotating-

wing aircraft with speeds up to 400 kilometers per hour
and more. The then-required coefficients of advance of 0.6
at around 180-meters-per-second tip speed are entirely
within the realms of possibility.

However, it is pointed out, at this opportunity, that
in the expressed high speed the performance of the rotat-
ing-wing aircraft is still likely always to be lower than
that of the fixed-wing aircraft because of the high coeffi-
cients of advance connected with it. The chief advantage
of the rotating-wing aircraft is that in spite of suffi-
cient maximum speed, it is able to reduce its forward
speed to the hovering stage. This quality will make it pref-
erable to the orthodox airplane for many practical purposes,
even if its top speed is lower.

DETERMINATION OF EFFICIENCIES

The calculation is based on the following substitute
functions for the aerodynamic force coefficients of the
blade element:

$$c_a = 5.6 \ \alpha_p \qquad\qquad\qquad\qquad\qquad (80)$$

$$c_w = 0.011 - 0.0572 \ \alpha_p + 0.89 \ \alpha_p^2 \qquad\qquad (81)$$

These data approximately correspond to the U.S. airfoil
M 12 at 1:30 aspect ratio. The parabola for c_w was
chosen so that at $\alpha_p = 0°$, $6.5°$, and $13°$ the substitute
function agrees with the true drag coefficient.*

The thrust-reduction factor B is - independent of
the propeller loading and blade number - put at 0.98; that
is, the outermost 2 percent of the rotor blade has no share
in the lift. For simplicity, it is further assumed that

---

*Since the downwash is already contained in λ_d when de-
termining the operating angles on the blade element - and
moreover, the polar for finite aspect ratio is employed -
the finite aspect ratio is allowed for, twice. The author
chose this method intentionally, since it is the simplest
way of obtaining agreement between theory and test. This
method, though very useful, is therefore merely an expedi-
ent until acceptable downwash measurements and the polars
of an airfoil under different angles of yaw make an exact
calculation possible.

the flapping hinge coincides with the axis of rotation.
The profile is the same as given in the earlier report
(T.M. No. 921). The hub resistance is ignored for the
present. The blade-mass constant on the rectangular blade
is put at $\gamma = 12$. A tapered blade 3:1 ($p = -\frac{2}{3}$) of the
same design which at 0.7R has the same chord as the rectan-
gular version, has about $\gamma = 23.4$. This value was then
used as the basis.

<center>Static-Thrust Coefficient</center>

For the hovering stage, the problem is to determine
the assumptions for an optimum static-thrust coefficient:

$$\eta = \frac{k_{sa}{}^{3/2}}{2k_d} \tag{82}$$

First to be defined is the most beneficial (specific) blade
loading k_{sa}/σ, which is an indication for an average op-
erating angle on the blade element.* This calculation was
made for an untwisted, rectangular blade by means of equa-
tions (11), (13), (14), and (82), and the data plotted
against the blade loading in figure 12 for different thrust
coefficients. The efficiency η rises with ascending
thrust coefficient to a maximum at $k_{sa}/\sigma = 0.195$ blade
loading, independent of k_{sa}.

The subsequent studies pertain to the improvement of
the efficiency by suitable blade design. For this analy-
sis, $k_{sa} = 0.009$ serves as a basis, which approximately
corresponds to the thrust coefficient of modern rotating-
wing aircraft.

Figure 13 shows the effect of twist on a rectangular
blade, with solidity σ as abscissa instead of the blade
loading. The best solidity in figure 13 is $\sigma \cong 5$ percent
for $k_{sa} = 0.009$, which again corresponds to ~ 0.2 blade
loading. It is also seen that a 12° twist raises the stat-
ic thrust coefficient from 67.8 to 74.8 percent, or 10.3
percent over the blade with zero twist.

---

*For the rectangular blade, equation (13) affords for the
average operating angle:

$$\alpha_p{}^\circ = \frac{3 \times 57.3}{c_a{}' B^3} k_{sa}/\sigma$$

$$\cong 32.6 \; k_{sa}/\sigma$$

As a general rule, the rotor blades will have only a little twist in consideration of forward flight and the autorotation ability endangered by a greater twist. In practice, therefore, the twist is not likely to exceed 8° to 10°.

A further means for improving the static-thrust efficiency is afforded by the taper of the blade; that is, taper of blade chord toward the tip. Here also the improvement is the result of a more uniform spanwise load distribution, the resultant of the tangential forces governing the torque traveling inward and thus becoming effective on a shorter lever arm.

Figure 14 illustrates the improvement afforded by a change from a simple rectangular blade to the untwisted and twisted tapered blade. The best solidity is again reached at 5 percent, that is, at a blade loading of $\frac{k_{sa}}{\sigma} \cong 0.2$, on the basis of 0.7R blade chord. According to figure 14, the efficiency by best solidity of 67.8 percent for a rectangular blade rises to 72.2 percent on the untwisted blade and to 77.6 percent on the tapered blade with 6 percent negative twist. The taper factor was $p = -\frac{2}{3}$; on a blade continuing to rotor center the chord of the innermost blade element to the theoretical chord (rounding off disregarded) at the blade tip the ratio would be as 3:1. This 6° twisted blade approximately corresponds to the blade form in modern designs.

To sum up, it may be stated that as regards hovering (without consideration to forward flight) a rotor of light blade loading with low tip speeds is propitious. A suitable blade loading is $k_{sa}/\sigma \cong 0.2$. With a twisted tapered blade, the efficiency can be improved by about 15 percent over a normal rectangular blade, which is about equivalent to a 10-percent lift increase by equal power input.

In the following, the optimum solidity is briefly discussed which, mathematically, does not become evident with the assumption $B = 0.98 = $ constant. Plotting the η values of figure 12 for the best blade loading $\frac{k_{sa}}{\sigma} = 0.2$ at the different thrust coefficients k_{sa} against the solidity (fig. 16) manifests a steady, slight rise in static-thrust coefficient with the solidity, which is not in accord with the facts.

Expressing the circulation decrease at the blade, conformable to Prandtl (reference 2)* with

$$B = 1 - \frac{\sqrt{k_{sa}}}{z}$$ (83)

gives the values shown in figure 15 in relation to k_{sa} for different blade numbers z and hence a maximum of the static-thrust efficiency, which is in accord with the tests at solidities of from 8 to 12 percent (fig. 16).

However, since the optimum is very weakly marked, a solidity of 6 percent is not likely to be exceeded because of the weight of the blades and their sagging on the stand. Even then it affords blades with sufficient static-thrust efficiency and adequate high speed.

Gliding Coefficient for Best Horizontal Flight

This implies the efficiency of the best possible horizontal flight; that is, the prediction of the normally attainable lowest gliding coefficient without regard to speed. We proceed from the coefficient of advance $\mu = 0.35$, that is, the value at which the best gliding coefficient may be expected, according to past information. The 280-kilometers-per-hour speed limitation connected with it, according to figure 11, is disregarded.

The solidity, in accord with modern designs, is put at $\sigma = 0.05$. This is the same value that gave the best static-thrust coefficient for $k_{sa} = 0.009$ in the hovering stage. The first task involves the determination of the best blade loading. Inasmuch as a change in blade loading at a given solidity is equivalent to a change in thrust coefficient, the coefficients of horizontal thrust and torque were computed for $k_{sa} = 0.005, 0.0075, 0.010$ (corresponding to a blade loading $k_{sa}/\sigma = 0.10, 0.15, 0.20$) and plotted against α (figs. 17 to 21), along with the blade angle of attack ϑ_0 necessary for each slope of the normal plane to produce the required thrust (lift).

---

*In equation (4), v is replaced by v_d, and v^2 in the denominator disregarded with respect to $R^2 \omega^2$. With $\lambda_d = \sqrt{k_{sa}}/1.4$, it affords

$$a = 1 - B = \frac{2 \ln 2}{1.4 \ z} \sqrt{k_{sa}}$$

$$B \cong 1 - \frac{\sqrt{k_{sa}}}{z}$$

Figures 17 to 19 show this result for a rotor with a rectangular blade of zero twist; and figures 20 and 21, for the best of the three explored blade loadings $k_{sa}/\sigma = 0.15$, based on a rectangular blade of $6°$ negative twist and a tapered blade $\left(p = -\frac{2}{3}\right)$ of zero twist.

The results were obtained in the following manner: λ_d is first obtained from the axial thrust equations (13) and (41) as functions of the blade loading and the blade angle of attack, respectively, and then written in the formulas for the torque and the normal thrust coefficients. With λ_d and k_{sa}, the related α value is afforded from equation (1), thus leaving the transformation of the coordinates to be effected. By this transition to the propeller - to the wind system, the calculation of k_{sh} (horizontal thrust) was made with $\cos \alpha = 1$, and the vertical put equal to the axial thrust (fig. 4). Since in the case of practical interest α_{max} reaches about $10°$ to $14°$, this omission has no significance so far as the result is concerned. Breakaway of flow was accounted for by $k_{sa}/\sigma = 0.15$ with $b = 0.7$, and by $k_{sa}/\sigma = 0.20$ with $b = 0.98$.

Further evaluation of the thus-obtained data consists in the calculation of the gliding coefficient ϵ, according to

$$\epsilon = \frac{k_{sh} + f \lambda^2}{k_{sv}} + \frac{k_d}{\lambda\, k_{sv}} \qquad (84)$$

where $f \lambda^2$ allows for the effect of additional resistance, such as fuselage, landing gear, and so forth. The factor f characterizes the ratio of parasite drag of all nonlifting parts of rotating-wing aircraft to swept rotor-disk area. All mechanical efficiencies of energy transmission and propeller efficiency are disregarded in equation (84) because of their subordinate role at this point.

In Part I (T.M. No. 921) it was stated that the required lift by equal rotor speed can be attained by different flight attitudes. The two extreme cases are briefly reviewed:

Autogiro: Up to about $5°$ blade angle of attack and positive setting of the normal plane relative to the air stream, the rotor is driven by the relative wind. A regular tractor propeller serves for overcoming the total drag.

Helicopter: The normal plane of a power-driven rotor
is tilted forward (negative α) until the rotor itself
overcomes its own drag and that of the aircraft. The
blade angles of attack must be increased to about $10°$ to
$12°$; a separate propeller is no longer required.

Figure 22 gives the efficiency of horizontal flight
by 0.35 coefficient of advance for these two extreme cases,
without allowing for additional drag. The curves show the
reciprocal gliding coefficient of a rotor with rectangular
blade of zero twist in relation to the blade loading.
For appraisal of the effect of twist and taper, the points
for a twisted, rectangular blade and a tapered blade of
zero twist have been added for $k_{sa}/\sigma = 0.15$. The helicop-
ter shows a temporary superiority over the autogiro for
f = 0. But, since a practical appraisal of the different
flight stages must take additive resistance into account
also, this comparison will be referred to again, later.

The best gliding coefficients for the autogiro with
simple - that is, rectangular blade of zero twist, lies at
$k_{sa}/\sigma = 0.16$; and for the helicopter at 0.14. In other
words, to maintain the best ϵ on changing from hovering
(best value at $k_{sa}/\sigma = 0.20$) to forward flight, theoretic-
ally requires an increase in rpm which, according to fig-
ure 22, should amount to 12 percent for the autogiro and
20 percent for the helicopter.

This well-known displacement of best blade loading on
autogiros is in accord with wind-tunnel test data. The
extensive measurements by Wheatley (reference 3) and eval-
uated by Hohenemser (reference 4) give, for instance, the
best gliding coefficients at $k_{sa}/\sigma = 0.15$ blade loading.
Corresponding helicopter tests are lacking.

For appraisal of the absolute values of the theoreti-
cal maximum efficiency of the helicopter, various full-
scale measurements, as reported by Cierva in a lecture be-
fore the Royal Aeronautical Society, on March 15, 1935
(reference 5) may be employed. According to this,
Wheatley's experiments on U.S. autogiro rotors yielded
gliding coefficients of from 1:8 to 1:10. These figures
would agree with the present calculation, which gives
1:8.4 as best value for the rectangular blade. The ta-
pered blade affords mathematically an improvement to about
1:9 - thus also falling into Wheatley's range of test val-
ues, which likewise include blade shapes differing from

the plain rectangular blade. It should be borne in mind
that on the tapered blade, with the same comparative so-
lidity $\sigma_{0.7}$, the decisive outer blade elements operate at
a lower characteristic coefficient than on the rectangu-
lar blade. Since this fact had not been taken into ac-
count in the calculation, the improvement in theoretical
gliding coefficient achieved here probably does not become
completely manifest. Cierva quotes $\epsilon = 1{:}13$ to $1{:}14$ as
optimum values obtained by himself. However, since nei-
ther these nor similar favorable gliding coefficients have
ever been definitely obtained up to now - neither by full-
scale nor on models - these figures seem a little too op-
timistic.

Obviously, the gliding coefficients usually obtained
in model tests, with a maximum of about $1{:}6$, are substan-
tially more unfavorable and not summarily applicable to
appraisals of optimum values obtainable at full scale.
This is chiefly due to the small characteristic values
and, in a lesser degree, to the additional losses usually
caused by the disproportionate dampers, hinges, and so
forth, which do not always lend themselves to satisfactory
mathematical treatment.

The effect of twist was illustrated on a rectangular
blade with negative twist ($\vartheta_1 = -6°$) for $k_{sa}/\sigma = 0.15$.
The gliding coefficient of the helicopter showed an im-
provement from $1{:}10.3$ to $1{:}10.9$. On the autogiro with op-
posed flow, this negative twist is detrimental because the
normal plane for the windmill state must be set too steep
as a result of the inferior autorotation ability.

The tapered blade affords an improvement on the auto-
giro as on the helicopter, with an absolute best value of
$\epsilon = 1{:}11$, computed on the basis of a blade taper of $3{:}1$
$\left(p = -\dfrac{2}{3}\right)$. With concurrent blade twist, this value pre-
sumably can be raised to about $1{:}12$ which, in the author's
opinion, is probably the upper limit for the present.

The effect of additional resistances is illustrated
in figure 23, where the reciprocal ϵ of a rotor is plot-
ted against the performance factor υ (characterization
of flight stage) for various parasite areas. The perform-
ance factor is defined as the ratio of rotor input power to
total power. Given the ϵ of a rotating-wing aircraft,
the performance factor υ can be computed according to

$$v = \frac{k_d}{\lambda \, \epsilon \, k_{sv}} \tag{85}$$

Figure 23 also shows the different angles of attack of the normal plane necessary to overcome the resistances of the aircraft in the helicopter state. The chosen representation has the advantage of placing for α = constant all potential flight stages on one straight line, which passes through the zero point of the coordinates with the inclination $\lambda \, k_{sv}/k_d$. The curves for ϵ were based on parasite areas of $f = 0.003$ and $f = 0.006$. The last value corresponds, for present-day dimensions, to a normal rotating-wing aircraft of the type of the C 30. $f = 0.003$ represents a particularly clean aerodynamic design. On the autogiro ($v = 0$) the parasite areas lower the gliding coefficient from 1:8.4 to 1:6.0 and 1:4.6, respectively. In the pure helicopter state ($v = 1$), ϵ is raised from 1:10.3 to 1:6.9 and 1:5.1, respectively. The forward tilt of the normal plane must, as a result of the additional resistances, be increased from $\alpha = -6.3°$ of the rotor windmill state to $-9.5°$ and $-12.7°$, respectively.

While the helicopter is superior for $f = 0$, the best ϵ for $f = 0.006$ lies with the helicogyro. Hence the superiority of the helicopter diminishes with increasing parasite drag relative to the other flight stages.

In the foregoing investigations the efficiency of the rotor drive and of a regular propeller required on occasion (autogiro or helicogyro) is disregarded. Since the gear efficiency is ordinarily substantially higher than the propeller efficiency, the helicopter superiority computed here is even more in evidence. This agrees with the flight tests of Focke's combined helicopter-autogiro, which attained the greater horizontal speed in the helicopter state.

CONCLUDING REMARKS

The best static thrust coefficients are obtained by blade loadings of $k_{sa}/\sigma = 0.2$, according to the study of the hovering state, and this figure can be raised by about 15 percent by using a tapered blade.

On passing from hovering to horizontal flight, the best blade loading for the explored coefficient of advance of

0.35 shifts to $k_{sa}/\sigma = 0.16$ for the autogiro and to $k_{sa}/\sigma = 0.14$ for the helicopter, hence the rpm should be increased.

The absolute best ϵ is to be expected at speeds below 300 kilometers per hour. It should amount to about 1:12 for the rotor without additional resistances when using a blade which is favorable for hovering also. A comparison of the different flight states gives for $\mu = 0.35$ in agreement with flight tests, a superiority of the helicopter which, though it may not be generalized, makes it likely that the helicopter, because of its superior take-off and landing characteristics, will be successful in the near future.

Since additional resistances are more detrimental to the gliding coefficient of the helicopter than on the autogiro, the greatest value for the helicopter should be placed upon an aerodynamically favorable design of the whole aircraft.

Translation by J. Vanier,
National Advisory Committee
for Aeronautics.

REFERENCES

1. Stack, John, and von Doenhoff, Albert E.: Tests of 16
    Related Airfoils at High Speeds. T.R. No. 492,
    NACA, 1934.

2. Prandtl, L., and Betz, A.: Vier Abhandlungen zur Hydro-
    dynamik und Aerodynamik, Nachsatz Prandtl zu Betz,
    Schraubenpropeller mit geringsten Energieverlust.
    Kaiser Wilhelm Instituts für Strömungsforschung,
    Göttingen, 1927.

3. Wheatley, John B., and Bioletti, Carlton: Wind-Tunnel
    Tests of 10-Foot-Diameter Autogiro Rotors. T.R.
    No. 552, NACA, 1936.

4. Hohenemser, K.: Performance of Rotating-Wing Aircraft.
    T.M. No. 871, NACA, 1938.

5. Cierva, Juan de la: New Developments of the Autogiro.
    Paper read before Society, March 15, 1935. Jour.
    R.A.S., Dec. 1935, pp. 1125-37.

XII. Tables

Table 1 (Fig. 12)

	k_{sa}/σ	$10^3 k_d$	$\eta\,\%$		k_{sa}/σ	$10^3 k_d$	$\eta\,\%$
$k_{sa}=0{,}003$	0,06	0,213	38,5	$k_{sa}=0{,}006$	0,06	0,495	46,9
	0,09	0,173	47,5		0,09	0,418	55,5
	0,12	0,156	52,6		0,12	0,384	60,4
	0,18	0,147	55,8		0,18	0,364	63,8
	0,24	0,148	55,5		0,24	0,368	63,0
	0,30	0,154	53,3		0,30	0,380	61,0

Table 1 (continued)

	k_{sa}/σ	$10^3 k_d$	$\eta\,\%$		k_{sa}/σ	$10^3 k_d$	$\eta\,\%$
$k_{sa}=0{,}009$	0,06	0,825	51,7	$k_{sa}=0{,}012$	0,06	1,195	55,0
	0,09	0,708	60,2		0,09	1,028	63,8
	0,12	0,659	64,7		0,12	0,970	67,7
	0,18	0,630	67,8		0,18	0,932	70,4
	0,24	0,635	67,2		0,24	0,938	70,0
	0,30	0,652	65,4		0,30	0,961	68,4

Table 2 (Fig 13)

k_{sa}	ϑ_1	p	σ	$10^3 k_d$	$\eta\,\%$
0,009	0	0	0,02	0,721	59,2
			0,03	0,651	65,5
			0,04	0,631	67,6
			0,05	0,628	67,8
			0,06	0,637	67,0
			0,07	0,650	65,6
			0,08	0,668	63,8
			0,10	0,708	60,2
			0,12	0,754	56,6
0,009	−6°	0	0,02	0,701	60,9
			0,03	0,627	68,0
			0,04	0,603	70,8
			0,05	0,598	71,3
			0,06	0,604	70,6
			0,07	0,614	69,5
			0,08	0,628	68,0
			0,10	0,663	64,5
			0,12	0,702	60,8
0,009	−12°	0	0,02	0,683	62,5
			0,03	0,606	70,5
			0,04	0,579	73,5
			0,05	0,571	74,7
			0,06	0,573	74,5
			0,07	0,581	73,5
			0,08	0,591	72,3
			0,10	0,620	68,8
			0,12	0,652	65,5

Table 8 (Fig. 14)

k_{sa}	ϑ_1	p	$\sigma_{0,7}$	$10^3 k_d$	$\eta\,\%$
0,009	0	0	0,02	0,721	59,2
			0,03	0,651	65,5
			0,04	0,631	67,6
			0,05	0,628	67,8
			0,06	0,637	67,0
			0,07	0,650	65,6
			0,08	0,668	63,8
			0,10	0,708	60,2
			0,12	0,754	56,6
0,009	0	−²/₃	0,02	0,685	62,2
			0,03	0,616	69,3
			0,04	0,593	71,8
			0,05	0,590	72,2
			0,06	0,595	71,6
			0,07	0,607	70,2
			0,08	0,621	68,7
			0,10	0,656	65,0
			0,12	0,697	61,1
0,009	−6°	−²/₃	0,02	0,659	64,8
			0,03	0,586	72,8
			0,04	0,559	76,3
			0,05	0,551	77,4
			0,06	0,553	77,2
			0,07	0,560	76,2
			0,08	0,570	74,9
			0,10	0,597	71,5
			0,12	0,628	67,9

Table 4.

|	ϑ_0	λ_d	α^0	$10^3 \cdot k_d$	$10^3 \cdot k_{sn}$	$10^3 \cdot k_{sh}$	
$k_{sa}/\sigma = 0{,}15,\ \vartheta_1 = 0^0,\ p = 0$	2	+ 0,0269	+ 5,3	− 0,089	+ 0,534	+ 1,255	Fig. 18
	5	− 0,0111	− 0,9	+ 0,081	+ 0,725	+ 0,602	
	8	− 0,0488	− 7,1	+ 0,291	+ 0,854	− 0,086	
	11	− 0,0868	− 13,1	+ 0,543	+ 0,920	− 0,782	
	14	− 0,1246	− 18,9	+ 0,837	+ 0,923	− 1,524	
$k_{sa}/\sigma = 0{,}15,\ \vartheta_1 = -6^0,\ p = 0$	6	+ 0,0290	+ 5,6	− 0,072	+ 0,456	+ 1,191	Fig. 20
	9	− 0,0092	− 0,6	+ 0,080	+ 0 668	+ 0,586	
	12	− 0,0470	− 6,8	+ 0,258	+ 0,818	− 0,074	
	15	− 0,0852	− 12,8	+ 0,455	+ 0,906	− 0,754	
	18	− 0,1232	− 19,4	+ 0,703	+ 0,931	− 1,569	
$k_{sa}/\sigma_{0,7} = 0{,}15,\ \vartheta_1 = 0^0,\ p = -²/₃$	2	+ 0,024	+ 4,8	− 0,032	+ 0,325	+ 0,955	Fig. 21
	4	+ 0,001	+ 1,0	+ 0,062	+ 0,504	+ 0,641	
	6	− 0,022	− 2,7	+ 0,159	+ 0,645	+ 0,289	
	8	− 0,045	− 6,5	+ 0,271	+ 0,750	− 0,105	
	10	− 0,068	− 10,1	+ 0,401	+ 0,818	− 0,502	
	12	− 0,091	− 13,8	+ 0,557	+ 0,849	− 0,931	
	14	− 0,114	− 17,3	+ 0,711	+ 0,844	− 1,391	
$k_{sa}/\sigma = 0{,}10,\ \vartheta_1 = 0^0,\ p = 0$	− 1	+ 0,0474	+ 8,3	− 0,042	+ 0,156	+ 0,886	Fig. 17
	1	+ 0,0220	+ 4,2	+ 0,015	+ 0,274	+ 0,639	
	3	− 0,0032	+ 0,1	+ 0,085	+ 0,364	+ 0,369	
	5	− 0,0288	− 4,1	+ 0,166	+ 0,426	+ 0,066	
	7	− 0,0538	− 8,2	+ 0,264	+ 0,461	− 0,259	
	9	− 0,0791	− 12,2	+ 0,375	+ 0,468	− 0,585	
	11	− 0,1043	− 16,1	+ 0,497	+ 0,447	− 0,938	
$k_{sa}/\sigma = 0{,}20,\ \vartheta_1 = 0^0,\ p = 0$	4	+ 0,0188	+ 4,3	− 0,139	+ 1,000	+ 1,742	Fig. 19
	6	− 0,0064	+ 0,1	+ 0,018	+ 1,163	+ 1,184	
	8	− 0,0318	− 4,1	+ 0,193	+ 1,299	+ 0,592	
	10	− 0,0571	− 8,1	+ 0,387	+ 1,409	− 0,020	
	12	− 0,0826	− 12,1	+ 0,600	+ 1,491	− 0,600	
	14	− 0,1076	− 16,0	+ 0,831	+ 1,545	− 1,215	
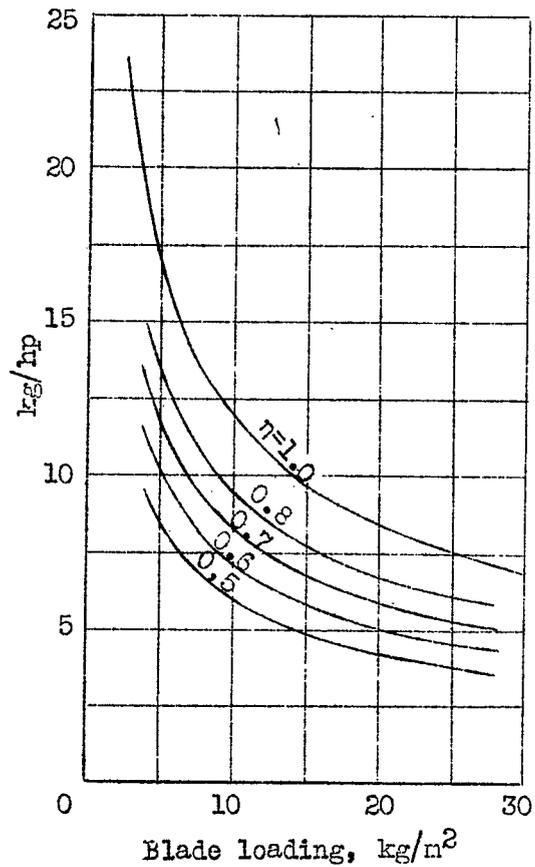
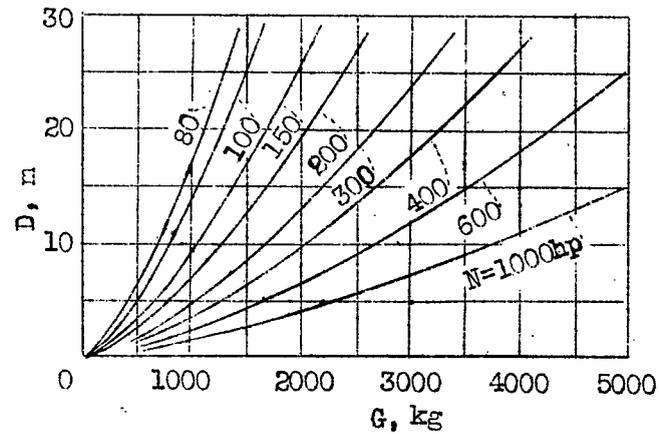Figure 8.— Thrust in hovering state
plotted against blade load-
ing.

Figure 9.— Minimum diameter of swept rotor
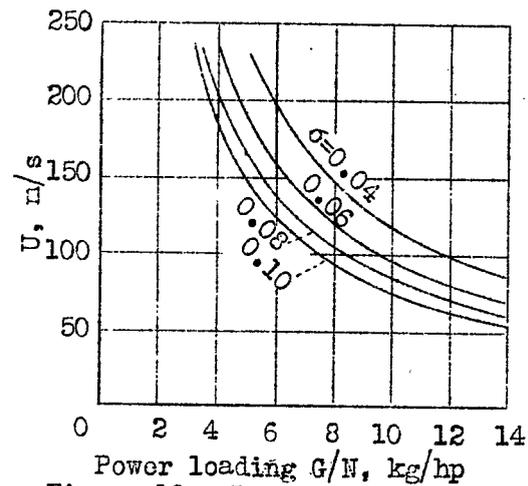disk for hovering.

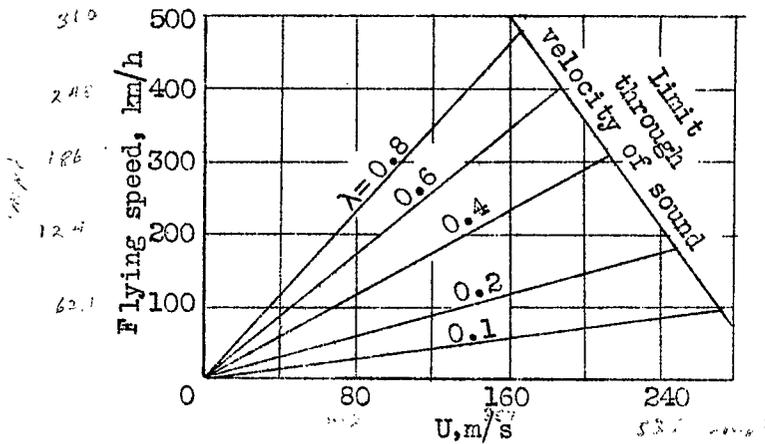Figure 10.— Best tip speed for
hovering.

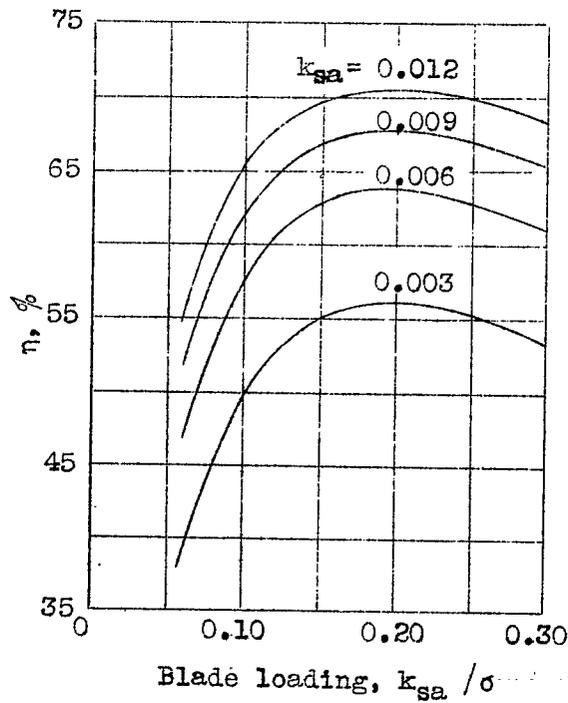Figure 11.- Speed limit at highest permissible Mach number of 0.9.

Figure 12.- Static thrust coefficient of plain rectangular blade.

Figure 13.

Static thrust coefficient of
rectangular blade improved
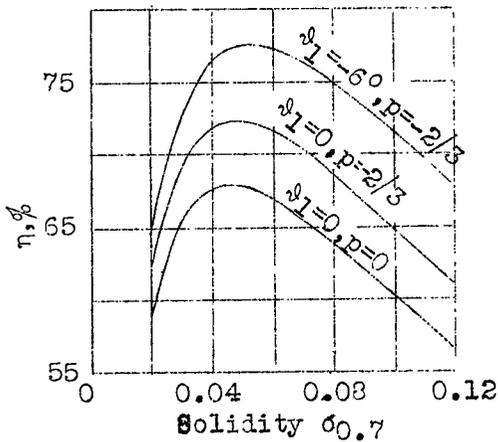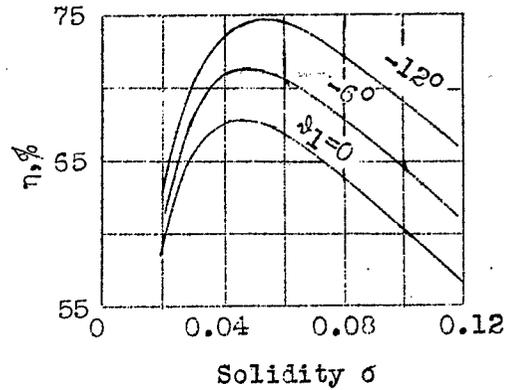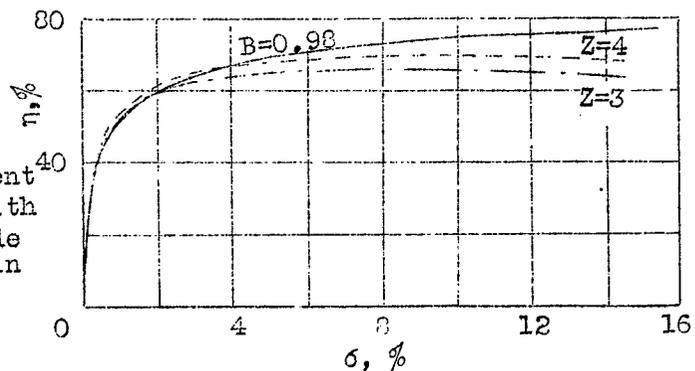by twist (k_{sa} = 0.009).

η, %

75

65

55

0   0.04   0.08   0.12

Solidity σ

$\vartheta_1 = -12^o$

-6°

$\vartheta_1 = 0$

Figure 14.

Static thrust coefficient improved
by changing from a simple rectan-
gular blade to a plain and a twist-
ed tapered blade (k_{sa} = 0.009).

η, %

75

65

55

0   0.04   0.08   0.12

Solidity $\sigma_{0.7}$

$\vartheta_1 = -6^o, p = -2/3$

$\vartheta_1 = 0, p = -2/3$

$\vartheta_1 = 0, p = 0$

Figure 16.

Static thrust coefficient
of rectangular blade with
zero twist by best blade
loading $\left(\dfrac{k_{sa}}{\sigma} = 0.2 \right)$ in
relation to solidity.

η, %

80

40

0   4   8   12   16

σ, %

B=0.98

Z=4

Z=3

$$\left(\frac{k_{sa}}{\sigma} = 0.10 \qquad \mu = 0.35\right)$$
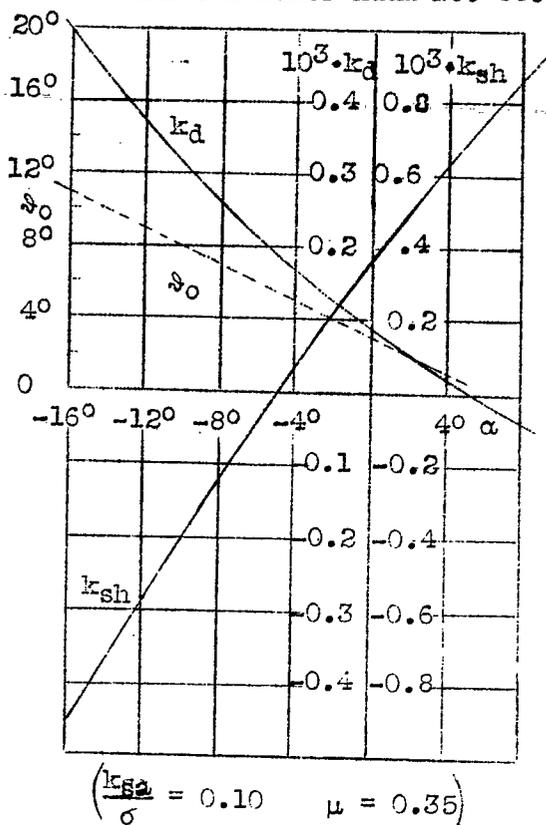
Figure 17.- Plain rectangular blade (no twist).

$$\left(\frac{k_{sa}}{\sigma} = 0.15 \qquad \mu = 0.35\right)$$
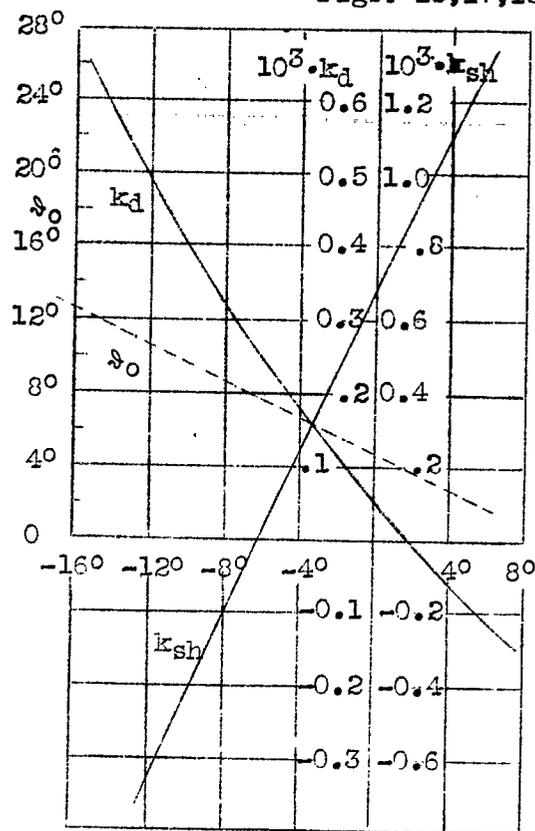
Figure 18.- Plain rectangular blade (no twist).

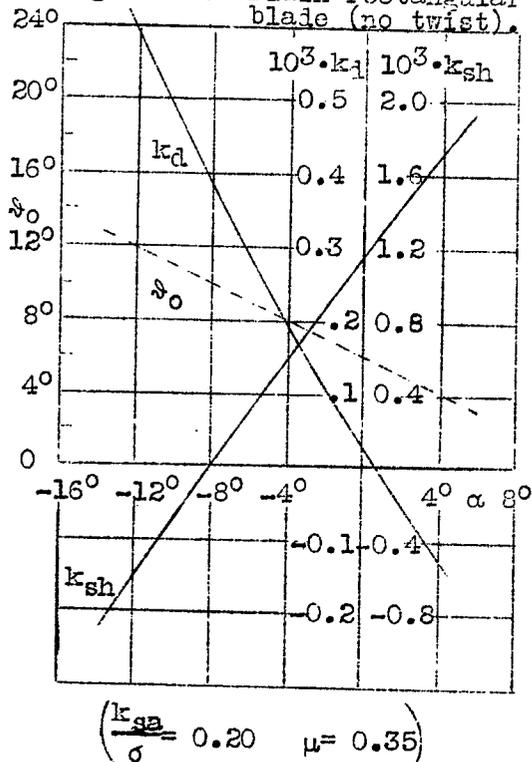$$\left(\frac{k_{sa}}{\sigma} = 0.20 \qquad \mu = 0.35\right)$$

Figure 19.- Plain rectangular blade (no twist).
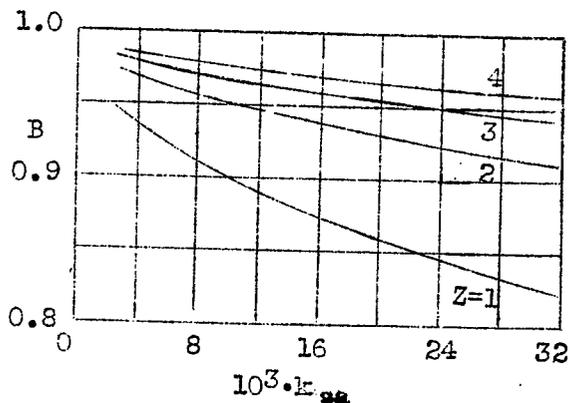
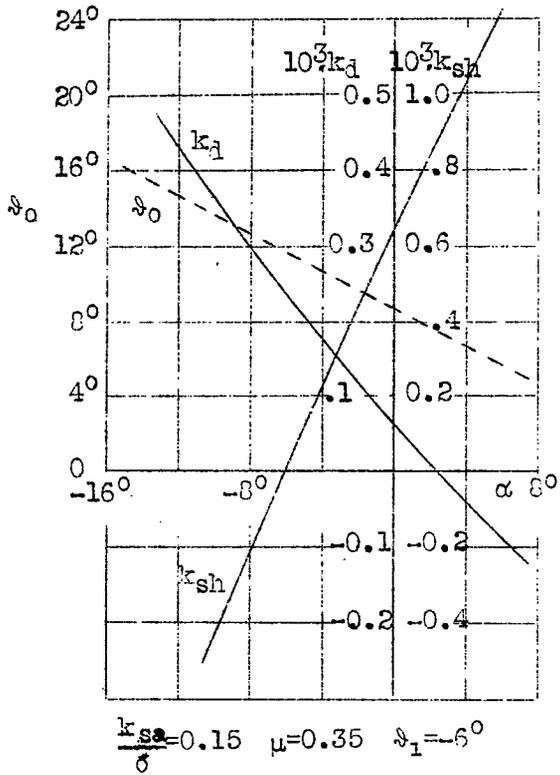Figure 15.- Effect of finite blade number and rotor loading on the thrust reduction factor B.

$\frac{k_{sa}}{\delta}=0.15$ $\mu=0.35$ $\vartheta_1=-6^\circ$

Figure 20.- Twisted rectangular
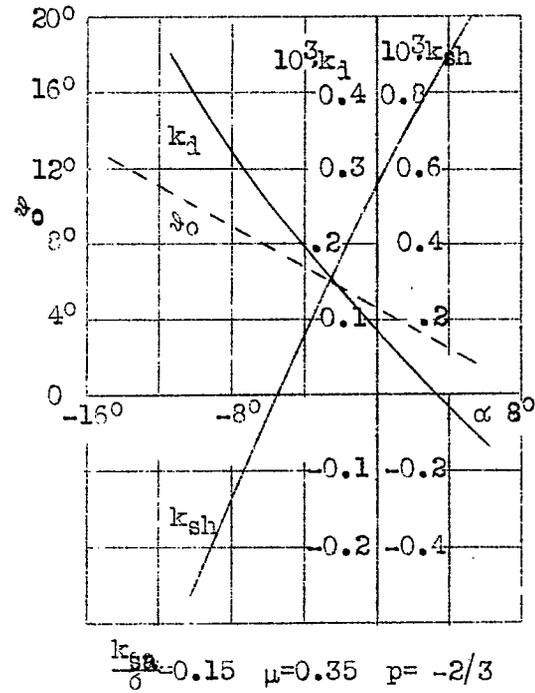blade.

$\frac{k_{sa}}{\delta}=0.15$ $\mu=0.35$ $p=-2/3$

Figure 21.- Tapered blade,
zero twist.
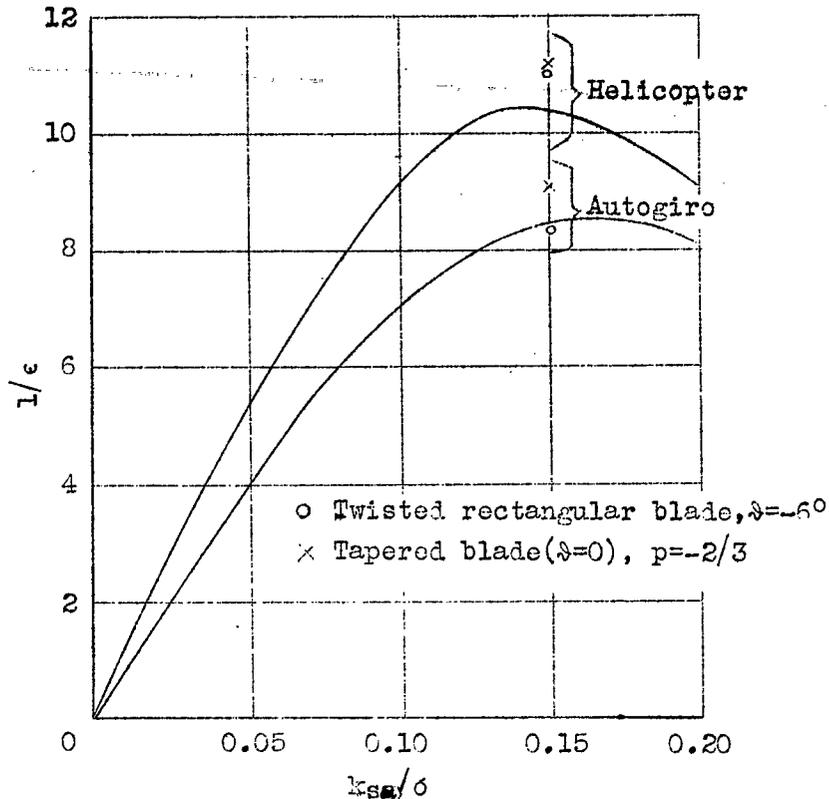
Figure 22.- Efficiency of rotor running
by itself (f=0) in autogiro
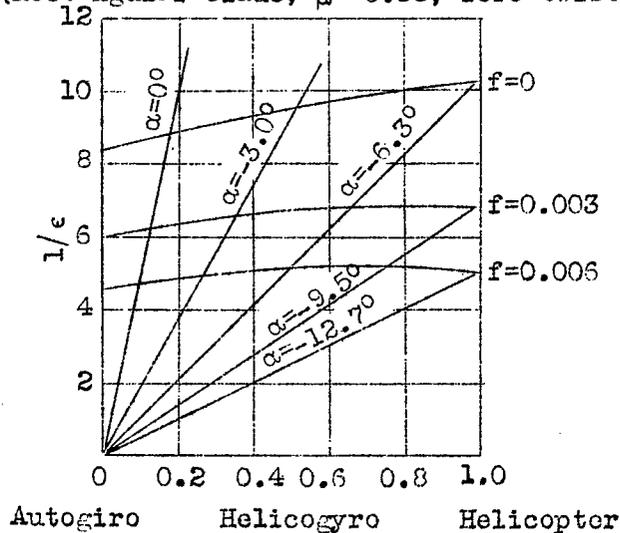and helicopter state.
(Rectangular blade, μ= 0.35, zero twist)

Figure 23.- Effect of equivalent parasite
area by μ= 0.35.
$\left[\text{Rectangular blade,} \dfrac{k_{sa}}{6} = 0.15, (\vartheta=0)\right]$